Generation of Intense Second Harmonic Light From Aperture Targets

Contact: ewan.bacon.2016@uni.strath.ac.uk

E.F.J. Bacon, M. King, R. Wilson,
T. P. Frazer, E. J. Dolier, M. Peat,
J. Goodman, R. J. Gray, P. McKenna
Department of Physics,
University of Strathclyde, Glasgow,
G1 1XQ, United Kingdom

T. Dzelzainis, C. Spindloe, S. Astbury
Central Laser Facility, STFC Rutherford Appleton Laboratory, Oxfordshire OX11 0QX, UK

1 Introduction

The advances made in laser technology over the past 4 decades have led to significant increases in the peak pulse intensity achievable [1], with multiple facilities able to produce pulses that far exceed the relativistic intensity threshold ($\geqslant 10^{18}$ Wcm^{-2} at a wavelength of 0.8 - 1 μm) [2][3][4]. Along with enabling the exploration of new regimes of laser-plasma interaction physics comes the issue of how to control and manipulate pulses of this intensity. When these pulses are transmitted through conventional solid state optics, non-linear effects such as self-phase modulation occur, negatively affecting pulse characteristics. One potential solution to this is the use of plasma based optics due to the ability of plasma to withstand extremely high energy fluences. This field of study is known as plasma optics or plasma photonics, with the control of pulse parameters such as polarisation [5], pulse duration [6] and temporal intensity contrast [7] having been investigated via either simulation or experiment. The control of the transverse spatial mode of a pulse at relativistic intensities is an active area of research, with the generation of so-called higher-order modes (HOM) at these intensities having various potential applications such as novel forms of electron and proton acceleration [8][9]. Examples of HOM include Laguerre-Gaussain (LG) and Hermite-Gaussian (HG) modes, shown in figure 1.

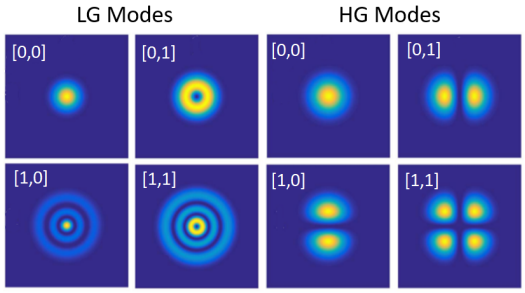

Figure 1: Examples of Higher Order Modes. Adapted from [10]

One mechanism for generating relativistically intense laser modes, shown in figure 2, involves the interaction between a high intensity pulse and an aperture target, generating a plasma at the aperture edges. As the pulse interacts with this plasma, electron bunches are accelerated from the aperture edges, emitting light as they do so in the form of a HOM. The electron bunches are emitted once per laser-cycle from each aperture edge, at opposite sides along the polarisation axis. Overall this leads to bunches being produced twice per laser cycle, meaning the generated HOM is composed of light with a frequency twice that of the drive pulse. The intensity of the generated light is around an order of magnitude below that of the drive pulse, enabling the HOM to exceed the relativistic threshold. The study of this mechanism leads on from experiments conducted by our group at Strathclyde involving the generation of a relativistic plasma aperture in an ultrathin foil undergoing transparency [14][12]. A similar mechanism has been reported on in [13].

This report provides a summary of the development of experimental methodologies to enable the investigation of this novel plasma-based mechanism for the generation of HOM at relativistic intensities, reported in [11], using the Gemini laser system in early 2022.

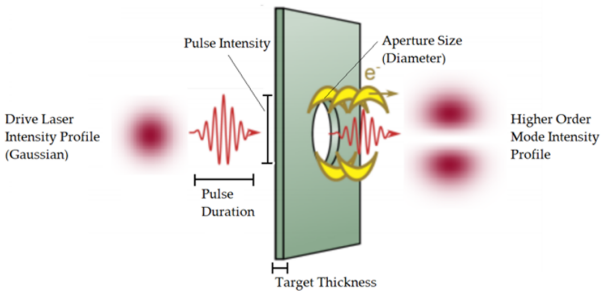

Figure 2: Schematic of the plasma-based HOM generation mechanism. Adapted from [11]

The numerical investigation of this mechanism was carried out prior to this experimental campaign, reported on in [11], with a selection of the relevant results

shown in figure 3. This includes the results of optimising the conversion efficiency of the mechanism, figure 3 (a), using 2D PIC simulations, by varying target thickness and aperture diameter, showing an optimum spot size (full-width at half-maximum; FWHM) to aperture size ratio, that being when these two values are equal. Shown in figure 3 (b) and (c) are examples of the use of circularly and linearly polarised light, respectively, to generate HOM, showing the dependency of the mode on pulse polarisation. These results proved to be useful in informing the direction of the experiment, giving us a range of parameters over which we could focus the investigation as well as predictions of the outcomes.

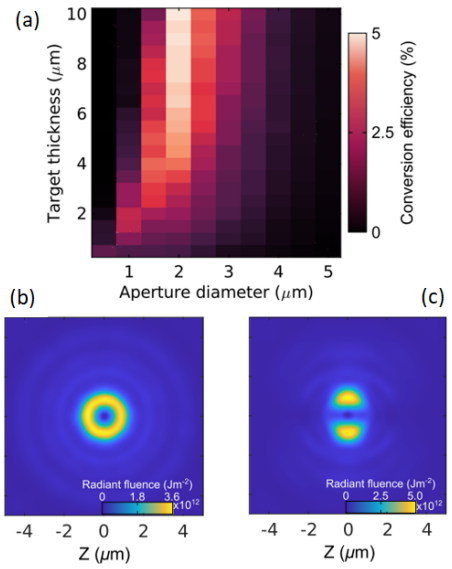

Figure 3: Results from the numerical investigation of the aperture mechanism, adapted from [11]. (a) Conversion efficiency from laser energy to 2ω light as a function of target thickness and aperture diameter. (b) and (c) HOM generated using a circularly and linearly polarised pulse, respectively.

2 Experimental Considerations

There were several obstacles to overcome experimentally. The first was how to mitigate the effects of the movement of the laser pulse between alignment to the target and a full-power shot, known as the on-shot spatial jitter of the laser pointing. Shown in figure 4 (a) and (b) are measurements of the movement of the focal spot in Y and X directions, respectively. These measurements were made from several hundred low-power shots using the Gemini system. From this it can be seen that it is possible for the focal spot to move up to $\backsim$ 3 μm in the Y direction and $\backsim$ 4 μm in the X direction. With the optimum focal spot size to aperture size ratio found via simulations to be when the two are equal and the focusing optic being used in the experiment providing a best focus of $\backsim$ 3 μm, this could lead to multiple shots missing the center of the aperture. One possible solution to this was to use a much larger focal spot size, achieved by moving the target past or into the focus of the beam. Knowing that the magnitude of the jitter remains the same, the negative effects of the on-shot spatial jitter would be greatly reduced. This was not seen as a viable option as increasing the focal spot size to this extent would reduce the intensity of the pulse, potentially below the relativistic threshold.

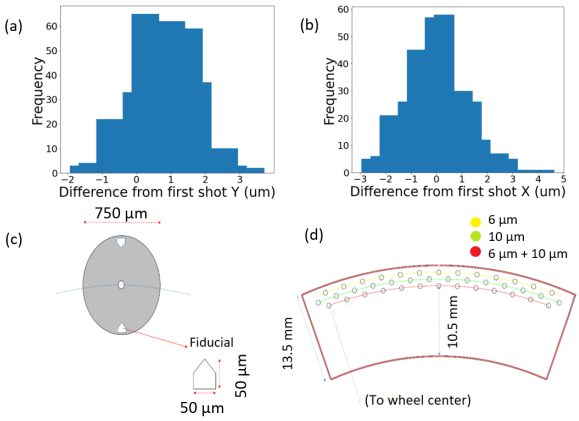

Figure 4: (a) and (b) are histograms of the movements of the focal spot between each shot in Y and X directions, respectively. (c) placement of a fiducial relative to an aperture. (d) segment of the target wheel developed for this experiment.

Knowing that it would be inevitable that a percentage of shots would miss the center of the apertures, the solution was to run the experiment at the maximum possible repetition rate. This would allow us to take a large enough number of shots such that there would be a statistically significant number of good shots (with the laser focus centred on the aperture). We could then determine whether a shot was a hit or a miss from other shot data such as the fractional transmission of the main pulse through the aperture. This provided two additional challenges, those being accurately aligning the aperture to laser focus due to their size and a target design which would facilitate high repetition rate operation through automated or precision target placement. By working with the Target Fabrication Group at the CLF, the solution was to include fiducial holes near the apertures, shown in figure 4 (c). Knowing the distance from the fiducial to the aperture enables the process of locating them to be expedited. To overcome the second problem, target fabrication was able to create multiple rows of targets on a single wafer of silicon, shown in figure 4 (d). Multiple of these wafers were then mounted on a drive system, forming a target wheel. The drive system allowed for the automated movement to a new target position after a shot, increasing the rep rate to the required level.

The targets themselves were made via process of etching, with an etching masked placed on top of the silicon wafers. While this was a relatively time consuming process, it provided high accuracy of aperture positioning and size, but limited the minimum aperture diameter to 6 μm.

3 Experimental Setup

The experiment was carried out in target area 3 (TA3) of the Gemini laser system, with a single plasma mirror setup employed to improve the temporal intensity contrast and two f/2 off-axis parabolas used to focus the pulse onto the aperture targets and then collect and collimate the generated light, with a schematic shown in figure 5. The focusing OAP created a spot size of 3 μm, with nominal pulse durations of 40 fs and on-target pulse energies of 5 J, leading to pulse intensities of around 3×10^{20} Wcm^{-2}. The laser was incident normal to the aperture targets. The main diagnostic used was a Stokes polarimeter to image the HOM produced. Along with this was a scatter screen to image transmitted near field light, placed behind the first wedge shown in figure 5, with CCD cameras filtered for both the fundamental frequency and frequency doubled light.

The aperture diameters were 6 μm and 10 μm with target thicknesses of 4 μm, 6 μm. These sizes were chosen based partly on the numerical investigation and the limitations of the manufacturing process. To vary the focal spot size, the targets were moved before focus, changing the size of the focal spot that interacted with the aperture. This enabled the spot size to aperture size ratio to be varied to investigate the trends predicted in the simulations.

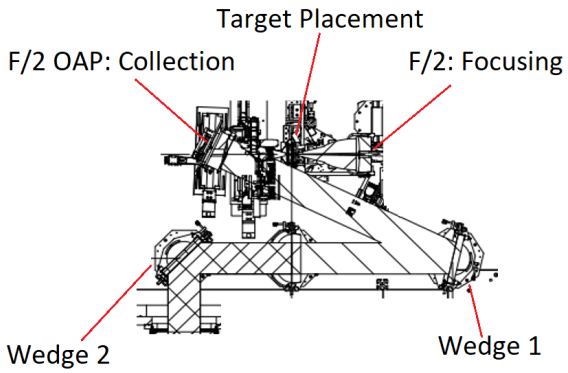

Figure 5: Schematic showing the experimental setup

4 Focal Spot Spatial-Intensity Profiles

During the experiment the focal spot to aperture size ratio was varied. As this was done, images of the focal spot were taken, with example images shown in figure 6. As can be seen, an increase in defocus led to a significant change in the spatial-intensity profile of the focal spot, with the greater the magnitude of defocus, the greater the deviation from the Gaussian profile seen at best-focus.

This change from Gaussian to non-Gaussian could have a significant effect on the HOM generation as the aperture edges will experience different pulse intensities, leading to a change in the quantity of light generated and the shape of the HOM produced. Preliminary analysis of the data shows a large amount of noise, so far attributed to both the on-shot spatial jitter and the variation in spatial-intensity profile.

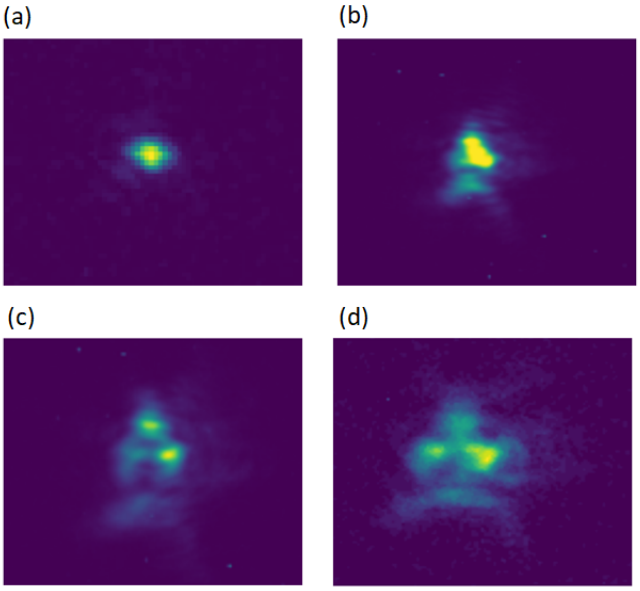

Figure 6: Images of the focal spot measurements made during the experiments for varying levels of defocus. (a) 0 μm (b) 29 μm (c) 45 μm (d) 60 μm

5 Conclusions

In summary, we have demonstrated an experimental capability to investigate the aperture targets proposed by our group [11][12] and others [13]. We have characterised expected sensitivities to on-shot spatial jitter and identified other key effects related to the change in the spatial-intensity profile of the laser as the focal spot size. This characterisation informed both this and future experimental campaigns involving aperture targets.

References

[1] G.A. Mourou et al. Exawatt-Zettawatt pulse generation and applications. *Optics communications* **285**, 5 (2012), p.720-724

[2] D. L. Balabanski et al. New light in nuclear physics: The extreme light infrastructure. *Europhysics Letters* **117**, 2 (2017), p.28001-28001
[3] E. I. Moses et al. The National Ignition Facility: Ushering in a new age for high energy density science. *Physics of Plasmas* **16**, 4 (2009), p.41006
[4] https://www.clf.stfc.ac.uk/Pages/EPAC-introduction-page.aspx
[5] S. Weng et al. Extreme case of Faraday effect: Magnetic splitting of ultrashort laser pulses in plasmas. *Optica* **4**, 9 (2017), p.1086-1091
[6] J. Ren et al. A new method for generating ultraintense and ultrashort laser pulses. *Nature Physics* **3**, 10 (2007), p.732–736
[7] C. Thaury et al. Plasma mirrors for ultrahigh-intensity optics. *Nature Physics* **3**, 6 (2007), p.424–429
[8] Y. Shi et al. Electron acceleration using twisted laser wavefronts. *Plasma physics and controlled fusion* **63**, 12 (2021), p.125032
[9] K. H. Pae et al. Low-divergence relativistic proton jet from a thin solid target driven by an ultra-intense circularly polarized Laguerre–Gaussian laser pulse. *Plasma physics and controlled fusion* **62**, 5 (2020), p.55009
[10] Rosales-Guzmán et al. Multiplexing 200 spatial modes with a single hologram. *Journal of optics* **19**, 11 (2017), p.113501
[11] E.F.J. Bacon et al. High order modes of intense second harmonic light produced from a plasma aperture. *Matter and Radiation at Extremes* **7**, 5 (2022)
[12] M.J. Duff et al. High order mode structure of intense light fields generated via a laser-driven relativistic plasma aperture. *Scientific reports* **10**, 1 (2020), p.105-105
[13] L. Yi . High-Harmonic Generation and Spin-Orbit Interaction of Light in a Relativistic Oscillating Window. *Physical review letters* **126**, 13 (2021), p.134801-134801
[14] B. Gonzalez-Izquierdo et al. Towards optical polarization control of laser-driven proton acceleration in foils undergoing relativistic transparency . *Nature Communications* **7**, 1 (2016), p.12891